

Investigation of the emitter structure in SiGe/Si resonant tunneling structures

G. Dehlinger^{a,*}, U. Gennser^a, D. Grützmacher^a, T. Ihn^b, E. Müller^a, K. Ensslin^b

^aPaul Scherrer Institute, CH-5232 Villigen PSI, Switzerland

^bSolid State Physics Laboratory, ETH Zürich, 8093 Zürich, Switzerland

Abstract

Pseudomorphically grown p-type Si/SiGe double barrier resonant tunneling diodes have been investigated. The main resonances are shown to be due to tunneling through heavy and light hole states in the well. However, temperature activated resonances and resonances arising in a *B*-field perpendicular to the current show the importance of the complicated emitter structure and its energy spectrum. © 2000 Elsevier Science S.A. All rights reserved.

Keywords: Molecular beam epitaxy; SiGe; Resonant tunneling devices

1. Introduction

Resonant tunneling devices (RTD) have attracted much attention over the years for their potential for fast devices [1] and, recently, as one of the constituent parts in the quantum cascade laser [2]. Due to the relatively large valence band offset in SiGe relative to Si, it is possible to realize RTD in the group IV material system. This was first demonstrated by Liu et al. [3] and by Rhee et al. [4] in 1988. It is possible to use either strained SiGe on a Si-substrate or strained Si on relaxed SiGe buffer layers. The first structure is limited to the critical thickness because of the strain, but the crystal perfection is not disturbed by dislocation formation. The flexibility in strain adjustment offers the possibility to study the physics of vertical hole transport in heterostructures. Earlier studies have focused on the role of the mixed heavy and light hole states in the well. Here we show that the emitter structure, which is rather complex in the pseudomorphic RTD due to the strain and accompanying thickness limitations, can have significant influence on the tunneling characteristics.

2. Experimental details

Double-barrier RTDs were grown pseudomorphically on heavily p-doped substrates using a Balzers UMS-500 molecular beam epitaxy (MBE), equipped with two e-gun evaporators for silicon and germanium and a boron effusion

cell. A typical layer sequence is shown in Fig. 1, together with a TEM-micrograph. A diode with symmetric spacer layer design consists typically of 50 Å barriers, a 50 Å well, 100 Å SiGe undoped spacers with constant Ge content on both sides, and SiGe ramps, ramping the Ge content from 5 to 26% on the substrate side and vice versa on the top side, of 150 Å, of which the inner 75 Å are also undoped. The Ge-content of the well and spacers is estimated to be 26%, deduced from separately grown SiGe superlattices and X-ray diffraction rocking curves. The Si-buffer and the cap layer are doped with boron at $2 \times 10^{18} \text{ cm}^{-3}$.

The growth temperature was varied between 250 and 600°C. All samples grown in this temperature range show resonances in the *I*–*V* or in the *dI/dV* characteristic. The best peak-to-valley ratio, ≈ 2 (taken at 4.2 K), was obtained at a growth temperature of 480°C.

The samples were processed by defining the mesa via photolithography, Al evaporation, lift-off, plasma etching and backside metallization. A short anneal was done for 10 s at 350°C. The size of the diodes ranged from 50×50 to $100 \times 100 \mu\text{m}^2$. The electrical characterization of the diodes was done at temperatures of 4–150 K using standard lock-in techniques.

3. Results and discussion

The valence band offset in our structures was estimated to be 230 meV for the heavy holes, calculated from data of [5]. The light hole band lies 50 meV above the heavy hole band due to strain splitting [6] and the two potentials lead to a

* Corresponding author.

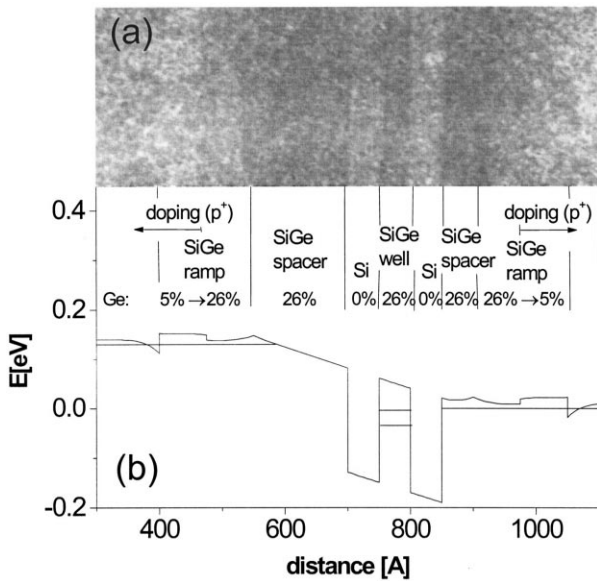


Fig. 1. (a) A TEM picture of a cross-section of one of a RTD with asymmetric spacer layers. (b) The layer sequence for a asymmetric RTD and the valence band edge calculated self-consistently for a bias of 130 mV, including heavy hole states only.

series of heavy hole (HH) and light hole (LH) quasi-bound states in the quantum well.

The resonances seen in the I - V characteristics (see Fig. 2) are attributed to resonant tunneling from the populated states in the emitter through the different states in the quantum well. The measured peak positions of a series of samples with varying well widths from 22 to 92 Å are shown in Fig. 3. There is a clear confinement shift as a function of the well width. The values are compared with calculated resonance voltages (solid lines) using a simple model of a particle in a box ($m^* \sim 0.19$) plus a lever arm factor (~ 4.2) for the potential drop in the collector region [7]. It is assumed that the whole undoped part of the collector is depleted, and the potential drop across the heterostructure is linear. This assumption agrees well with self-

consistent calculations using a Poisson solver. In view of the simplicity of the model, there is a very good correlation between the experimental and calculated resonances, especially for the first heavy hole level (HH1). The discrepancy is somewhat larger for the higher lying states. This may be due to ignoring the potential drop across the quantum well, as well as a small series contact resistance, the influence of which increases with the conductance of the diode. Levels may also come down due to leakage through the barriers which increases with increasing energy of the state. Or the lever arm may change due to depletion in the collector.

Though these results agree well with the simple model outlined above, a closer inspection of the temperature dependence as well as the magnetotunneling characteristics reveals that the energy spectrum in the emitter also has to be taken into account. The temperature dependence was investigated in detail for a selection of these diodes, using a cold finger cryostat with temperatures of 20–120 K. For these samples the negative differential resistance (NDR) disappears above 50 K. The resonances weaken with increasing temperature. The strongest one, the first light hole level, can be seen in the derivative up to 120 K.

In contrast to this general behavior, a different peak, not detected at the lowest temperatures, develops on the low bias side of the HH1 as the temperature is increased above ca. 20 K. It can be seen in different samples and lies 30–50 mV (corresponding to 10–15 meV) below the HH1, (see Fig. 4). Matutinovic-Krstelj et al. [8], have reported a somewhat similar resonance that appears below the first resonance at high temperatures in an n-type Si/SiGe RTD.

In order to analyze the behavior of the two resonances, after removing the exponential non-resonant current background, they have been fitted with two Gaussian peaks. The height of the activated resonance can be Arrhenius plotted, yielding an activation energy of ≈ 2 meV.

The fact that the temperature activated resonance occurs at lower voltages than the first resonance excludes any phonon emission related resonance, but in view of the energy level spacing in the SiGe quantum well a possible

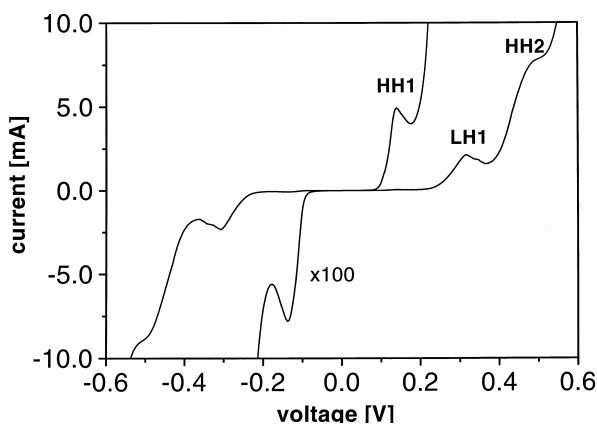


Fig. 2. I - V curve of a typical symmetric RTD at 4 K. The low voltage region is enlarged by a factor of 100 to show the HH1 peak.

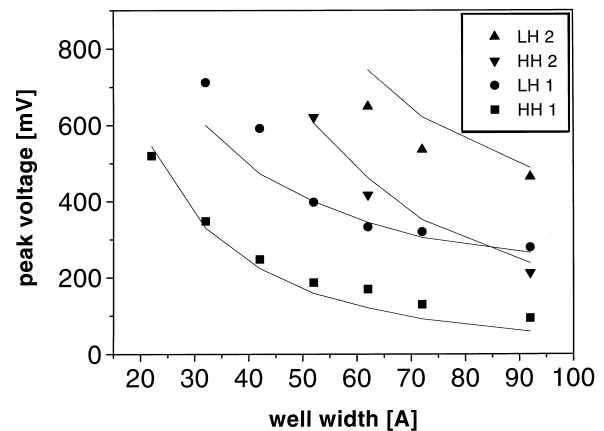


Fig. 3. Confinement shift vs. well width for a series of RTDs; dots indicate the measured resonance-positions and the solid lines the calculated values.

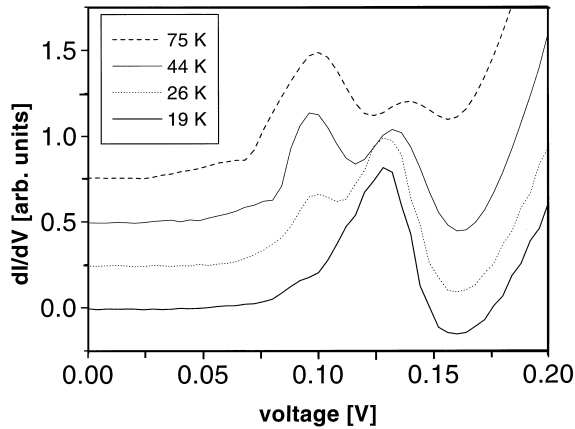


Fig. 4. Conductance of the temperature dependence of the first resonance. It clearly shows the developing peak on the left shoulder of the HH1 peak. The curves are vertically shifted for clarity.

path could be the absorption of an optical phonon and tunneling through the LH1 state, situated ca. 60 meV above the temperature activated resonance. However, the observed temperature dependence contradicts such a path and predicts a state much closer to the Fermi-level. A possible tunneling path may be from excited levels in the emitter through the HH1 quantum well state. As can be seen in Fig. 1, the potential of the spacer layer is quite irregular. In fact, the self-consistent calculation shows that it can form a shallow but 20 nm wide quantum well due to the Ge onset, the end of the doping and a triangular shaped potential drop due to the applied bias. We estimate a Fermi-energy of $E_F \approx 11$ meV above the valence band edge in the silicon layers, taking into account the anisotropic light and heavy hole effective masses. Calculations show two energy levels in the emitter well below E_F , and a third level a few meV above E_F , which can be populated by thermally excited holes. This level is severely broadened. However, the resulting modulation of the density of states may still be sufficient to explain the temperature activated resonance, as verified by model calculations of the current.

The onset of the HH1 resonance (see Fig. 4; this is seen at 0.08 V at 19 K) appears when the Fermi level reaches the quantum well state. Assuming that the temperature activated resonance is due to holes, tunneling from an emitter state above the Fermi energy into a sharp HH1 state, this resonance would appear at lower voltages than the HH1 onset at low temperatures. However, as the resonance develops at higher voltages, this indicates that the well level is broadened. A ± 2 Å fluctuation in the well, (which is a reasonable number, as the growth temperature was in a region, where the Ge segregation is expected to be at its maximum), will lead to a broadening of ca. 5 meV of the first state, which agrees well with the voltage difference between the HH1 onset current and the position of the temperature activated resonance.

Though this model does not exclude other possibilities, for example tunneling from a defect state in the emitter, it

shows the possibility of tunneling from an excited quasi-bound emitter state through the QW state.

We now turn to the measurements in a magnetic field. Previous investigations have shown, that magneto-tunneling experiments can be a useful spectroscopy tool [9–11] of the valence band quantum well states. We have studied the tunneling in fields up to 8 T perpendicular to the current. The magnetic field adds a momentum to the tunneling holes, i.e. it shifts the emitter k -space parabola relative to the well state. This makes it possible to map out the dispersion of the hole state [9]. The relatively small fields used here only give rise to small voltage shifts of the resonances, which makes it difficult to compare the results with the calculated dispersion relations. However, they agree qualitatively with the magnetic field dependence reported on for RTD grown by atmospheric pressure CVD [11]. It is clear that the HH shift less to higher bias voltages than the LH-level (see Fig. 5; for a field of 8 T the shifts are 1–2 meV for the HH1, ca. 11 meV for the LH1 and ca. 7 meV for the HH2).

In several of the samples an extra resonance develops with a perpendicular magnetic field, but in contrast to the temperature activated resonance, it lies ca 8 meV above the HH1 and increases with magnetic field. The shift with magnetic field is only 1–2 meV at 8 T. The existence of such a peak has been reported elsewhere [12], and it was speculated that the spacer-width plays an important role for the appearance of this peak. To further investigate this idea we have grown a series of samples with varying spacer-layer widths. The part with constant Ge content was varied between 50 and 200 Å, in addition to asymmetric samples with different spacer widths on both sides. In Fig. 5 the dI/dV - V curves for different magnetic fields are shown for an asymmetric structure (spacer width 50/150 Å). The resonances at the negative bias appear at lower voltages due to the smaller lever arm factor. However, in addition to this asymmetry, the field induced resonance appears only on the side with the smaller spacer (labeled 'B' in Fig. 5).

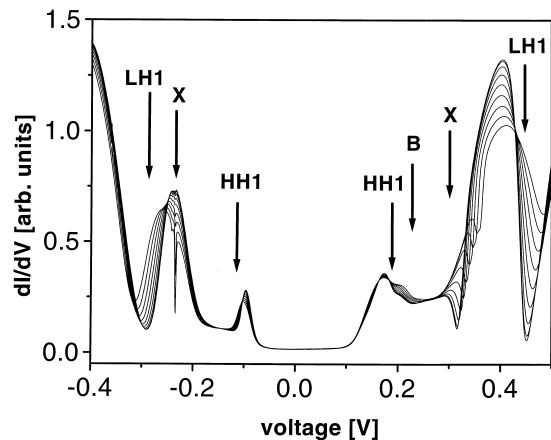


Fig. 5. B -field dependence of the conductance of an asymmetric RTD in magnetic field from 0 to 8 T, measured at 1.7 K. The B -field induced resonance on the positive bias side is marked with 'B', the extra resonances are marked with 'X'.

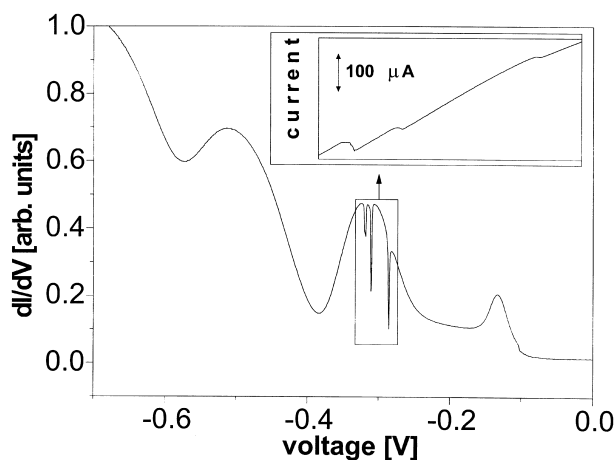


Fig. 6. Series of very sharp resonances in some devices clearly exhibits NDR, but disappear completely above 50 K (measured at 1.7 K).

This is generally true for the asymmetric samples. We hope that future investigations at higher B -fields may clarify if the resonance ‘B’ is related to strain and a B -field induced resonance reported in [11].

In addition to the main resonances (see Fig. 2), some of the devices also exhibits other, often much sharper resonances, lying between HH1 and LH1. These can not be explained by the simple picture of holes tunneling from the emitter through the quantized states in the quantum well. They do not show a uniform shape or behavior with B -field (labeled ‘X’ in Fig. 3).

In two of the samples there are series of features, separated by a few meV and of widths <1 meV. They show NDR at low temperature, but disappear completely at temperatures above 50 K, i.e. at much lower temperatures than the ‘normal’ resonances (Fig. 6).

A possible explanation is that these resonances are due to tunneling through defect states such as impurities or dislocations. Such defects, localized in one of the barriers, may explain the different behavior in the two bias directions. The localization in k -space may also explain the sudden decrease in current, when the state is shifted below the emitter ground state.

4. Conclusion

RTD with varying parameters have been grown using MBE. Confinement shifts, as a function of the well width, verify that the resonances are due to tunneling through heavy hole and light hole states in the well. However, the temperature dependence of the I - V characteristics, the measurements in magnetic fields up to 8 T, and measurements with different spacer layer widths show the importance of the emitter energy spectrum for the tunneling characteristics. We show that this can lead to additional temperature activated and B -field induced resonances. Furthermore, additional sharp resonances in the I - V characteristics were seen, which may be attributed to tunneling through defect states.

References

- [1] F. Capasso, S. Datta, *Phys. Today* 43 (1990) 74.
- [2] J. Faist, F. Capasso, D.L. Sivco, C. Sirtori, A.L. Hutchinson, A.Y. Cho, *Science* 264 (1994) 553.
- [3] H.C. Liu, D. Landheer, M. Buchanan, D.C. Houghton, *Appl. Phys. Lett.* 52 (1988) 1809.
- [4] S.S. Rhee, J.S. Park, R.P.G. Karunasiri, Q. Ye, K.L. Wang, *Appl. Phys. Lett.* 53 (1988) 204.
- [5] D.J. Robbins, L.T. Canham, S.J. Barnett, A.D. Pitt, P. Calcott, *J. Appl. Phys.* 71 (1992) 1407.
- [6] C.G. Van de Walle, Properties of strained and relaxed silicon and germanium, in: E. Kaspar (Ed.), *EMIS Data Reviews Series No. 12*, INSPEC, IEE, 1995.
- [7] G. Schuberth, G. Abstreiter, E. Gornik, F. Schäffler, J.F. Luy, *Phys. Rev. B* 43 (1991) 2280.
- [8] Z. Matutinovic-Krstelj, C.W. Liu, X. Xiao, J.C. Sturm, *Appl. Phys. Lett.* 62 (1993) 603.
- [9] R.K. Hayden, D.K. Maude, L. Eaves, et al., *Phys. Rev. Lett.* 66 (1991) 1749.
- [10] U. Gennser, V.P. Kesan, D.A. Syphers, T.P. Smith, S.S. Iyer, E.S. Yang, *Phys. Rev. Lett.* 67 (1991) 1749.
- [11] A. Zaslavsky, T.P. Smith, D.A. Grützmacher, S.Y. Lin, T.O. Sedgwick, *Phys. Rev. B* 48 (1993) 15112.
- [12] P. Gassot, U. Gennser, D.M. Symons, A. Zaslavsky, D.A. Grützmacher, J.C. Portal, *Phys. E* 2 (1998) 758.